Short communication

Synthesis and assay of retro-α4β1 integrin-targeting motifs

Samantha D. Dattoli [b], Rossella De Marco [a], Monica Baiula [b], Santi Spampinato [b], Arianna Greco [a], Alessandra Tolomelli [a], Luca Gentilucci [a],*

[a] Dept. of Chemistry "G. Ciamician", University of Bologna, via Selmi 2, 40126 Bologna, Italy
[b] Dept. of Pharmacy and BioTechnology, University of Bologna, via Irnerio 48, 40126 Bologna, Italy

ABSTRACT

In recent years, several research groups proposed new peptidomimetic antagonists of integrins αvβ3, α5β1, αIIbβ3, αvβ6, αvβ5, etc. based on retro sequences of the classic integrin-binding motif RGD. The retro strategy is still largely ignored for the non-RGD-binding α4β1 integrin. Herein we present the first examples of retro sequences for targeting this integrin, composed of Asp or *iso*Asp equipped with an aromatic cap at the *N*-terminus, (*S*)-pyrrolidine-3-carboxylic acid (β²-Pro) as a constrained core, and the amino variant (AMPUMP) of the well-known α4-targeting diphenylurea MPUPA. We discuss α4β1 receptor affinity (SPA), cell adhesion assays, stability in mouse serum, and conformational analysis. For their significant ability to inhibit cell adhesion and remarkable stability, the retro-peptide mimetics BnCO-Asp-β-Pro-AMPUMP (**3**) and BnCO-*iso*Asp-β-Pro-AMPUMP (**4**) represent promising candidates for designing small molecules as potential anti-inflammatory agents.

© 2013 Elsevier Masson SAS. All rights reserved.

1. Introduction

The integrin α4β1 (VLA-4, very late activation antigen-4, CD49d/CD29) is a cell surface receptor expressed on lymphocytes (and also on monocytes, eosinophils, basophils, macrophages), that mediates cellular adhesion events crucial to leukocyte trafficking and activation during inflammatory processes [1,2]. If the condition becomes chronic, there can be a sustained extravasation of lymphocytes that can exacerbate the inflammatory condition, which in turn will continue to recruit more inflammatory cells resulting in tissue destruction.

Their involvement in disease processes prompted several pharmaceutical companies to pursue α4 integrin antagonists as potential anti-inflammatory agents [3]. Monoclonal α4 integrin

antibodies have been shown to be modulators in animal models for auto-inflammatory diseases such as asthma, rheumatoid arthritis, and inflammatory bowel diseases [4,5]. The humanized monoclonal antibody Natalizumab has been approved for multiple sclerosis [5]. However, the inherent limitations of antibody therapy, high cost, potential immunogenicity, and the requirement for intravenous administration, strongly spurred efforts to develop small molecule antagonists.
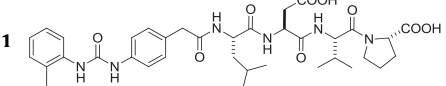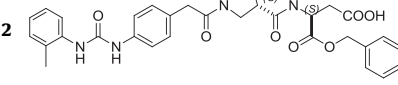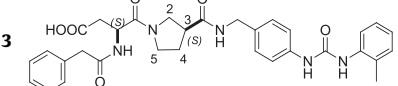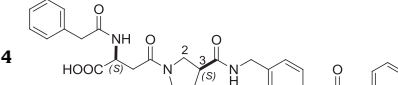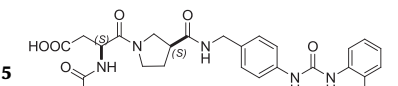
The primary ligands of α4β1 integrin are vascular cell adhesion molecule (VCAM) and the extracellular matrix (ECM) protein fibronectin (FN). Their integrin-binding sites contain a critical aspartic acid located within a highly conserved tripeptide sequences, Ile-Asp-Ser (IDS) in VCAM and Leu-Asp-Val (LDV) in FN [6,7]. Consequently, peptidomimetics and non-peptide mimetics of the recognition sequences can effectively inhibit the integrin [6,7]. For instance, the combination of a LDVP sequence and *N*-terminal *o*-methylphenylureaphenylacetyl group (MPUPA) leads to the potent selective BIO1211 (MPUPA-LDVP-OH **1**, Table 1) [8–10]. However, the residual peptidic nature of **1** and related compounds resulted in rapid enzymatic hydrolysis [11,12] and clearance in vivo [13]. Among the non-peptides, the *N*-(2,6-diclorobenzoyl)-2,6-dimethoxy biphenylalanine TR-14035 was highlighted as a non-specific α4 integrin antagonist [14]. In general, the large majority of the peptidomimetic compounds share common structural

Table 1
SPA binding to bead-associated α4β1 integrin and inhibition of Jurkat cell adhesion of BIO1211 (**1**) and compounds **2**–**6**.[a]

	Structure	Purity (%)[b]	m/z [M + 1] vs calcd	SPA IC50 (nM)	SPA Ki (nM)	α4β1/VCAM-1 IC50 (nM)	αvβ3/VT IC50 (nM)
1		–		4.80 ± 2.4	1.50 ± 0.37	7.60 ± 3.0	–
2		96	587.2/587.2	>10^5	>10^5	>10^5	–
3		98	586.2/586.3	100 ± 40	60 ± 10	80 ± 10	>10^5
4		97	586.1/586.3	290 ± 20	180 ± 40	93 ± 10	>10^5
5		96	640.1/640.2	3.90 ± 0.54 × 10^3	2.4 ± 0.25 × 10^3	>10^5	–
6		96	640.1/640.2	>10^5	>10^5	>10^5	–

[a] Mean of four determinations ± SE.
[b] Determined by analytical RP-HPLC; see Materials and instruments.

features: a α4-targeting aromatic cap at the *N*-terminus (eventually an aromatic urea such as MPUPA), a suitable spacer, and a β-carboxylate mimetic of Asp [6,7].

In search for new lead structures, the similarities between the different types of integrins prompted several research groups to test the Arg-Gly-Asp (RGD) sequence for inhibition of α4β1. This epitope, discovered several years earlier, was found on numerous ECM proteins, collagen, fibrinogen, vitronectin (VT), and FN, and was known to interact with several integrins, including αvβ3, α5β1, αIIbβ3, etc [15]. Mould et al. described the ability of peptide GRGDS and homologs to inhibit the interaction of α4β1 with the alternatively spliced type III connecting segment (IIICS) region of fibronectin [16], and Cardarelli et al. provided evidence that RGD-containing cyclopeptide 1-adamantaneacetyl-CGRGDSPC(S-S) [17] was a inhibitor of cell adhesion mediated by α4β1. Also, Nowlin, Cardarelli, et al. showed that the RCD-containing cyclic peptide RCD(ThioP)C(S-S) inhibited α4β1 and α5β1 integrin-mediated cell adhesion [18], and Jackson et al. observed that cyclic peptides containing RCD blocked the interaction of α4β1 with VCAM-1 [19]. Using atomic force microscopy measurement of monocyte–endothelial cell interaction, Elitok et al. demonstrated that a cRGD peptide inhibited their adhesion through α4β1-VCAM-1, resulting in the inhibition of monocyte/macrophage infiltration [20].

Albeit the α4β1 receptor was not definitively documented to interact RGD peptides with high affinity, these results suggest that the strategies successfully developed for designing a variety of RGD-derived analogs [21,22] could potentially be used to identify new α4β1 antagonists [6,7]. In this respect, we sought to investigate

the opportunity to design retro sequences of the common MPUPA-spacer-Asp peptidomimetic-binding motif (see above) of the integrin α4β1 as potential antagonists. In the last few years, the use of retro sequences of the classic RGD-binding motif for αvβ3 and α5β1-integrin has became popular. Initially, Kessler et al. investigated the biological activity of retro (DGR), inverso (rGd), retro–inverso (dGr) analogs (plus their stereoisomers) of the selective and superactive αvβ3 integrin inhibitor c[RGDfV] [23]. Some years later, we proposed cyclopeptides containing the partially modified retro Arg-Gly-Asp sequence ψ(NHCO)Aspψ-(NHCO)Gly-Arg [24]. Novellino, Kessler, et al., grafted the *iso*DGR motif onto c[phg-*iso*DGRG], achieving activity enhancement toward α5β1 integrin [25,26]; further, selectivity toward FN-binding integrins α5β1 and αvβ6 over VT-binding integrins αvβ3 and αvβ5 was improved changing the flanking amino acids [26].

Some researchers have proposed that deamidation of the Asn-Gly-Arg (NGR) motif in FN into *iso*DGR might result in a gain of protein function by creating a new adhesion binding site for integrins [27,28]. However, this hypothesis was questioned in a report using recombinant FN with mutations in the NGR motif [29]. Later investigations suggested that the *iso*DGR sequence can fit into the RGD-binding pocket of integrin, establishing the same electrostatic clamp as well as additional polar interactions [30–32].

These considerations prompted us to transfer the retro strategy into peptidomimetic sequences showing Asp or *iso*Asp, a central spacer, and the amino variant 1-(4-(aminomethyl)phenyl)-3-(o-methylphenyl)urea (AMPUMP) of the well-known α4-targeting
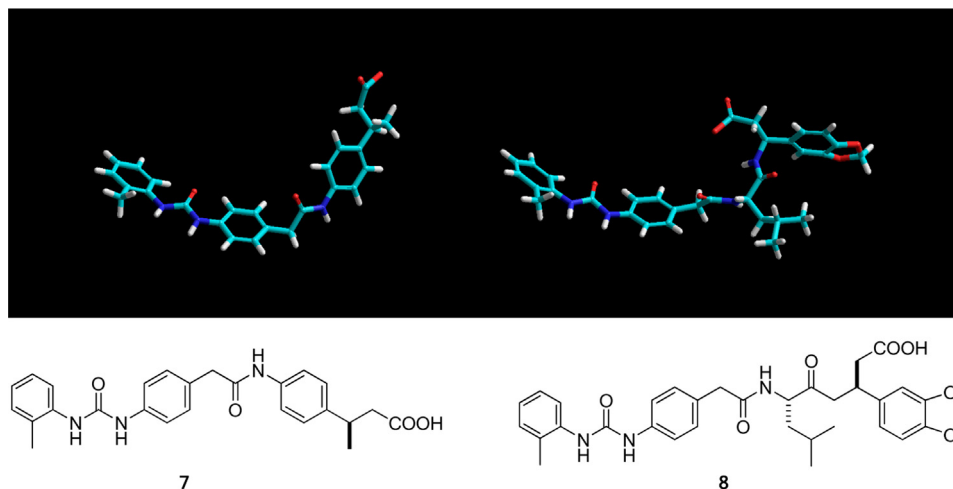
Fig. 1. Structures of the model compounds **7** (and top, left) and **8** (and top, right) as reported in the literature.

MPUPA, giving the retro sequences Asp-spacer-AMPUMP and *iso*-Asp-spacer-AMPUMP [6—10].

2. Results and discussion

2.1. Design and synthesis

The structures of the peptidomimetics **2**—**6** (Table 1) were designed on the basis of the models developed by 3D-QSAR analysis of large libraries of compounds containing diphenylureas such as MPUPA, or other substituted aromatic groups [13,33,34]. 3D geometries of plausible candidates were screened prior to synthesis by molecular modeling [35]; Fig. 1 shows the bioactive geometries and structures of the prototypic model compounds **7** [13,36] and **8** [2,33]. This selection led to the retro sequences Asp-β^2-Pro-AMPUMP **3** and **5**, and *iso*Asp-β^2-Pro-AMPUMP **4** and **6** (β^2-Pro, (S)-pyrrolidine-3-carboxylic acid). The straight sequence MPUPA-β^2-Pro-Asp **2** was considered for comparison, and BIO1211 (MPUPA-Leu-Asp-Val-Pro-OH, **1**) was chosen as $\alpha4\beta1$ integrin antagonist reference compound.

The sequences **2**—**6** were assembled by connecting β^2-Pro to MPUPA or AMPUMP. The β^2-Pro core was chosen to increase peptide stability [37], and for the conformational control exerted on the overall structure [38—41]. Further, we took advantage of our previous experience in the use of β^2-Pro or equivalent heterocycles [42] for preparing highly stable peptidomimetics [43], including

highly active integrin ligands [44]. Asp and *iso*Asp were equipped with aromatic substituents; it is well known that the presence of an aromatic moiety adjacent to Asp can favor integrin binding [6,7]. The compounds **3** and **4** show a phenylacetyl *N*-cap (BnCO), while **5** and **6** include the *N*-2,6-dichlorobenzoyl group, which was shown to efficiently bind to the $\beta1$-subunit [45], and is present in many ligands, including TR-14035 [6,7,14]. After synthesis and bioassay, the coherence of the most active compounds with the geometries of the 3D-QSAR models was confirmed by 2D ROESY and molecular dynamics (see Section 2.5).

As a representative example, the preparation of the BnCO-*iso*Asp-β^2-Pro-AMPUMP sequence **4** is described in Scheme 1; for the details on the intermediates, see Supporting Material (S.M.). Fmoc-Asp(O*t*-Bu)-OH was treated with BnBr, giving **9**, and Fmoc was replaced with the phenylacetyl group *via* **10**. The resulting fully protected Asp **11** was treated with TFA giving **12**. In parallel, Boc-4-(aminomethyl)aniline was treated with 2-methylbenzene isocyanate affording Boc-AMPUMP **13**. This was treated with TFA, and resulting AMPUMP **14** was coupled with Boc-β-Pro-OH in solution under MW irradiation and in the presence of HOBt/HBTU/DIPEA, giving **15**. Boc deprotection was followed by coupling with **12** under the same conditions as before. The resulting **17** was deprotected by catalytic hydrogenation, giving **4** in very good yield. The strategies for the syntheses of the remaining compounds are given in S.M. The products were purified (96—98%) by semipreparative reversed-phase (RP) HPLC.
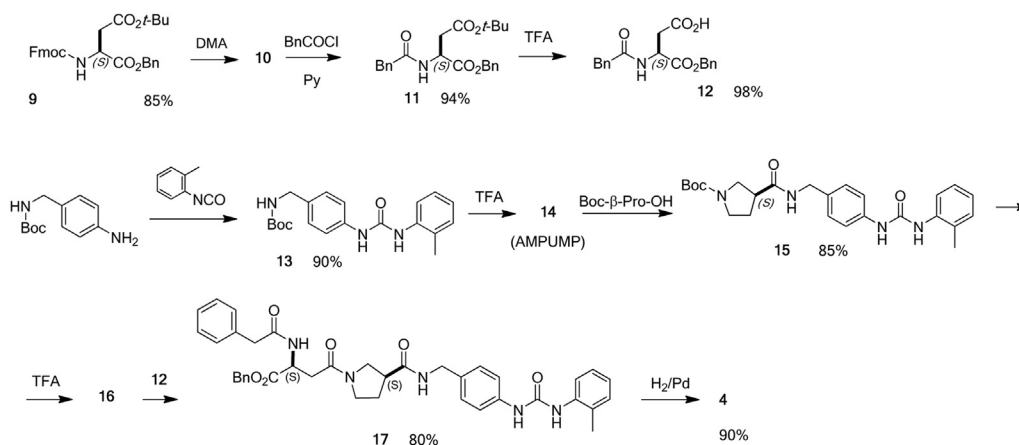
Scheme 1. Synthesis of BnCO-*iso*Asp-β^2-Pro-AMPUMP (**4**).

2.2. Scintillation proximity-binding assay

The binding of the peptidomimetics **1**–**6** to α4β1 integrin was measured by (SPA), using Jurkat cells stably expressing human α4 integrin, and ^{125}I-FN as the specific radioligand [46,47]. Western blot analysis of the α4β1 integrin, extracted from cell lysate and purified by chromatography, confirmed that both α4 and β1 integrin subunits were present in the eluate employed for the test (S.M.).

Specific binding of ^{125}I-FN to an antibody-captured α4 and β1 integrin was time-dependent; the signal reached a plateau in 10 h and remained constant for the rest of the 24 h incubation (S.M.). The relatively slow kinetics of the SPA may require the establishment of equilibrium between the different components [46,47]. ^{125}I-FN specific binding to the SPA bead-associated α4β1 integrin, measured after overnight incubation, was inhibited in a concentration-dependent manner by BIO1211, MPUMP-Leu-Asp-Val-Pro-OH (**1**), with IC_{50} and K_i values of 4.8 and 1.5 nM, respectively (Table 1). Furthermore, ^{125}I-FN selective binding was blocked by an anti-human α4 integrin antibody (5 mg/tube) to capture the integrin complex (data not shown).

The straight sequence MPUMP-β²-Pro-Asp-OBn **2** was not able to inhibit ^{125}I-FN binding. On the contrary, the retro compounds **3**–**5** caused concentration-dependent inhibition of ^{125}I-FN binding (Table 1). The sequence BnCO-Asp-β²-Pro-AMPUMP **3** showed IC_{50} and K_i values (M) of 1.0×10^{-7} and 6.0×10^{-8}, respectively. The analog of **3** containing *iso*Asp **4** showed IC_{50} of 2.9×10^{-7} and K_i of 1.8×10^{-7} M. The analog of **3** equipped with the 2,6-dicholorobenzoyl group **5** revealed a modest affinity, in the micromolar range, while **6**, analog of **4** with the 2,6-dicholorobenzoyl instead of the phenylacetyl (BnCO) group, did not displace ^{125}I-FN in a significant way.

2.3. Cell adhesion inhibition

Subsequently, we assayed the ability of **1**–**6** to inhibit the adhesion of α4β1 integrin-expressing Jurkat cells to VCAM-1. In a first series of experiments, we ascertained that adhesion of these cells to 96-well plates coated with human recombinant VCAM-1 was concentration-dependent and was not observed in BSA-coated wells [46,47]. The adhesion of Jurkat cells (5×10^5 cells per well) to VCAM-1 (2–25 mg/mL) ranged from 1.9 to 3.2×10^4 cells. The adhesion to VCAM-1 (10 mg/mL) was inhibited (>92%) after pretreatment with 5 mg/mL of an anti-α4 integrin antibody. As shown in Table 1, the reference compound BIO1211 (MPUPA-Leu-Asp-Val-Pro-OH, **1**) behaved as a potent α4β1 integrin ligand and inhibited Jurkat cell adhesion to VCAM-1 with a IC_{50} of 7.6 nM. Peptidomimetics **2** and **6** did not affect cell adhesion to a significant extent, confirming the results of the SPA assay. Interestingly, the retro compounds BnCO-Asp-β²-Pro-AMPUMP (**3**) and BnCO-*iso*-Asp-β²-Pro-AMPUMP (**4**) inhibited cell adhesion with an IC_{50} of 80 and 93 nM, respectively. On the contrary, **5** failed to behave as adhesion antagonist, despite of the micromolar affinity revealed by the SPA (Table 1). In addition, **3** and **4** did not show any significant activity ($IC_{50} > 100$ μM) in cell adhesion assays (Table 1) aimed to evaluate any potential antagonist activity toward αvβ3 integrin (SK-MEL-24 cells coated with 10 mg/mL VT). Finally, neither compound (up to 2 mM) influenced cell viability, evaluated by Trypan blue exclusion (data not shown).

2.4. In vitro metabolic stability

BIO1211 (**1**) was found to be very unstable in heparinized blood, plasma and rat liver, lung and intestinal homogenates, being metabolized by hydrolytic cleavage of the terminal dipeptide moiety, giving a sequence [11,12] much less active than the parent compound [8]. For their peptidomimetic nature the sequences BnCO-Asp-β²-Pro-urea **3** and BnCO-*iso*Asp-β²-Pro-urea **4** were supposed to be significantly more stable, in particular for the presence of the central β-Pro. The resistance of **3** and **4** to enzymatic degradation was estimated using 100% mouse serum (Sigma) [48] and compared to that of **1** under the same conditions. After 120 min, **3** was degraded to a moderate extent (about 10%), and **4** was only slightly degraded (<5%) after incubation in the mouse serum, while **1** was almost completely hydrolyzed, being present only in traces, as detected by RP-HPLC and ESI-MS analyses. Apparently, the presence of *iso*Asp increased the stability of **4** compared to **3**.

2.5. Conformational analyses

The significant biological activity of the structurally correlated BnCO-Asp-β²-Pro-AMPUMP (**3**) and BnCO-*iso*Asp-β²-Pro-AMPUMP (**4**) prompted us to analyze the conformations by NMR spectroscopy and MD simulations (S.M.), in particular to check the fulfillment of the geometric requisites of the 3D models utilized for structure design (Section 2.1).

As expected on the basis of the literature [38–41], the ^{1}H NMR of both **3** and **4** revealed two sets of resonances, in about 1:1 ratio, corresponding to the cis and trans conformers of the peptide bond linking the pyrrolidine ring. The cis conformations were assigned by detection of the NOE cross peaks between AspHα (**3**) or *iso*AspHβ (**4**) and PyrrolidineH-2, while the trans conformations were deduced by detection of the NOE cross peaks between AspHα (**3**) or *iso*AspHβ (**4**) and PyrrolidineH-5 (for this numbering, see the structures **3** and **4** in Table 1, and structures associated to Tables S1–S4) [49].

Molecular conformations were investigated by 2D ROESY in 8:2 DMSO-d_6/H₂O; DMSO-d_6 alone or mixtures of DMSO-d_6 and H₂O have been recommended by several authors as biomimetic media [50,51]. Cross-peak intensities were ranked to infer plausible inter-proton distances as restraints. Structures consistent with ROESY were obtained by simulated annealing with restrained MD [35] in a box of explicit TIP3P water molecules. The structures were minimized with the AMBER force field and clustered by the rmsd analysis of backbone atoms (S.M.).

For **3**, computations essentially gave one major cluster for the all-trans conformer and one cluster for the trans-cis-trans conformer, each comprising almost 95% of the structures. For each cluster, the representative geometries all-trans-**3**A and trans-

Fig. 2. Representative low-energy structure all-trans-**3**A (**3**, BnCO-Asp-β²-Pro-AMPUMP) consistent with ROESY analysis and calculated by restrained MD; alternative minor conformer **3**B (low-energy structure), determined by unrestrained MD; representative low-energy structure of trans-cis-trans-**3**C calculated by restrained MD; minor conformer **3**D (low-energy structure) determined by unrestrained MD. All structures obtained in a 45 × 45 × 45 Å box of standard TIP3P water molecules.

cis-trans-**3**C with the lowest internal energy and no violations of the distance constraints were selected and analyzed (Fig. 2).

To investigate the dynamic behavior, the structures **3**A and **3**C were analyzed by unrestrained MD for 10 ns in a $45 \times 45 \times 45$ Å box of explicit, equilibrated water molecules. Besides to the all-trans-**3**A, the analysis of the trajectories revealed the occurrence of the minor all-trans conformer **3**B, differing almost exclusively in the orientation of BnCO-Asp-β-Pro dipeptide respect to the AMPUMP group. The analysis of the trajectories of trans-cis-trans-**3**C revealed the presence of the minor conformer **3**D, showing the alternative orientation of BnCO-Asp-β-Pro respect to AMPUMP (Fig. 2). On the other hand, the conversion of the all-trans conformers into the trans-cis-trans conformers was observed very seldom.

In a similar way, computations for **4** gave one cluster for the all-trans conformer and one cluster for the trans-cis-trans conformer (>90% of the structures). Fig. 3 shows the representative low-energy geometries of all-trans-**4**A and trans-cis-trans-**4**C. Unrestrained MD performed as described for **3** revealed the alternative minor conformers all-trans-**4**B and trans-cis-trans-**4**D, differing from **4**A and **4**C in the display of the Asp-β-Pro dipeptide respect to the AMPUMP group.

Despite of potentially high flexibility of the linear ligands, the β-Pro scaffold conferred them markedly bent conformations. Indeed, the conformers **A** and **C** determined by restrained MD were clearly predominant during the unrestrained MD simulations in water. Apparently, both all-trans-**A** and trans-cis-trans-**C** conformations seemed compatible with one or the other 3D model **7** or **8** (Fig. 1) [2,13, 33,36,52,53]. For the moment, the determination of the different contribution of the cis and trans geometries to the bioactive conformations of the compounds is not possible.

The most significant differences between the corresponding conformations of **3** and **4** were related to the position of the aromatic group adjacent to Asp or *iso*Asp, respectively. This might be correlated to the slightly different IC_{50} and K_i values determined by SPA, confirming the role of the flanking aromatic substituent for efficient binding of the receptor [23–25,33].

3. Conclusion

In summary, we have presented the first implementation of the retro-sequence strategy for the design of new α4β1 integrin inhibitors. Starting from the well-known α4β1 integrin-binding motif "MPUPA-spacer-Asp", exemplified by the potent and selective ligand BIO1211 (MPUPA-Leu-Asp-Val-Pro-OH), we assembled the retro peptidomimetic sequences by connecting Asp or *iso*Asp, and the amino variant (AMPUMP) of the widely utilized diphenylurea MPUPA, to a pyrrolidine-3-carboxylate (β²-Pro) scaffold, the latter selected by inspection of the 3D models (3D-QSAR) reported in the literature. After syntheses, the conformational analyses confirmed the good agreement with the models.

Interestingly, while the straight sequence MPUPA-β-Pro-Asp-OBn (**2**), analog of BIO1211, was completely inactive, the retro sequences BnCO-Asp-β-Pro-AMPUMP (**3**) and BnCO-*iso*Asp-β-Pro-AMPUMP (**4**), displayed a moderate binding affinity (SPA), and efficiently inhibited the adhesion of α4β1 integrin-expressing cells to VCAM-1. Besides, the peptidomimetic nature conferred to these compounds good in vitro metabolic stability (mouse serum). Albeit **3** was a slightly more potent inhibitor than **4**, the latter was significantly more stable. These evidences support that the retro approach can furnish promising candidates for the development of a new class of peptidomimetic anti-inflammatory agents.

4. Experiments

4.1. Materials and instruments

Unless stated otherwise, chemicals were obtained from commercial sources and used without further purification. The MW-assisted synthesis was performed using a MicroSYNTH microwave labstation. Flash chromatography was performed on silica-gel (230–400 mesh), using mixtures of distilled solvents. Purities were determined to be ≥96% by analytical RP-HPLC and combustion analysis. Analytical RP-HPLC was performed on an C18 column (4.6 µm particle size, 100 Å pore diameter, 250 µm, DAD 210 nm, from a 9:1 H_2O/CH_3CN to a 2:8 H_2O/CH_3CN, with the addition of 0.05% TFA, in 20 min) at a flow rate of 1.0 mL/min, followed by 10 min at the same composition. Elemental analyses were performed using a Thermo Flash 2000 CHNS/O analyzer. Semi-preparative RP-HPLC was performed on a C18 column (7 µm particle size, 21.2 mm × 150 mm, from 8:2 H_2O/CH_3CN to 100% CH_3CN, with the addition of 0.05% TFA, in 10 min) at a flow rate of 12 mL/min. Mass analysis was done by ESI. ^{1}H NMR and ^{13}C NMR spectra were recorded at 400 and 100 MHz, respectively, in 5 mm tubes, at rt. Chemical shifts are reported as δ values relative to the solvent peak. 2D spectra were recorded in the phase sensitive mode and processed using a 90°-shifted, squared sinebell apodization.

4.2. Peptide coupling, general procedure

HOBt (1.1 mmol) and HBTU (1.1 mmol) were added to a stirred solution of the acid partner (1.0 mmol) in 4:1 DCM/DMF (5 mL) at rt under inert atmosphere. After 5 min, the amino partner-TFA salt (1.1 mmol) and DIPEA (2.2 mmol) were added at rt, and the mixture was stirred under MW irradiation, keeping irradiation power fixed at 150 W and monitoring the internal reaction temperature at 80 °C with a built-in ATC-FO advanced fiber optic automatic temperature control. After 10 min the mixture was diluted with DCM, and the solution was washed with 0.5 M HCl (5 mL) and with a saturated solution of NaHCO₃ (5 mL). The organic layer was dried over Na₂SO₄, and solvent was removed at reduced pressure. The intermediates were isolated by crystallization from EtOH/Et₂O or by flash chromatography over silica-gel. For the preparation of the different Asp or *iso*Asp derivatives and of **11**, see S.M. Compounds **2**–**6** were purified by semipreparative RP-HPLC (see 4.1. Materials and instruments) (70–85% yield, 96–98% pure by analytical RP-HPLC).

2. ^{1}H NMR (CDCl₃) δ (ppm): (two sets of resonances: ≥major conformer; ≤minor conformer) 1.95 (m, 1H, PyrrolidineH-4), 2.05–
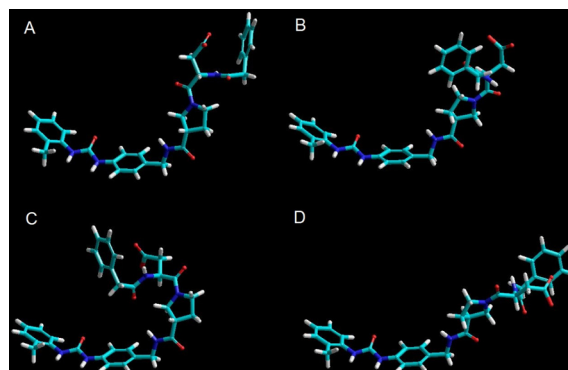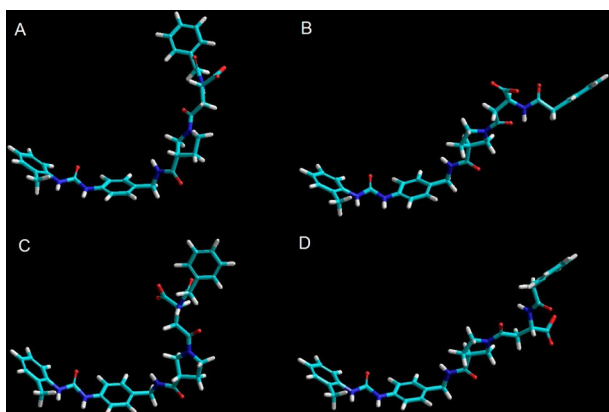

Fig. 3. Representative low-energy structure all-trans-**4**A (**4**, BnCO-*iso*Asp-β²-Pro-AMPUMP) consistent with ROESY analysis and calculated by restrained MD; alternative minor conformer **4**B (low-energy structure), determined by unrestrained MD; representative low-energy structure of trans-cis-trans-**4**C calculated by restrained MD; minor conformer **4**D (low-energy structure) determined by unrestrained MD. All structures obtained in a $45 \times 45 \times 45$ Å box of standard TIP3P water molecules.

2.19 (m, 4H, CH$_3$ + PyrrolidineH-4), 2.74 (m, 1H, AspHβ), 2.90–2.99 (m, 2H, PyrrolidineH-3 + AspHβ), 3.36 (m, 2H, PyrrolidineH-5$_<$ + PyrrolidineH-2$_>$), 3.41–3.50 (m, 2H, PyrrolidineH-2$_>$ + PyrrolidineH-5$_<$), 3.54 (d, J = 5.2 Hz, 2H, ArCH$_2$CON), 3.51–3.60 (m, 4H, PyrrolidineH-2$_<$ + PyrrolidineH-5$_>$), 4.78 (m, 1H, AspHα), 5.07 (br.s, 2H, CH$_2$Ph), 6.96 (t, J = 7.6 Hz, 1H, ArH), 7.00–7.08 (m, 3H, ArH), 7.09–7.18 (m, 5H, ArH), 7.24–7.32 (m, 4H, ArH + NH), 7.35 (d, J = 8.8 Hz, 1H, AspNH), 7.56 (s, 1H, NH), 7.60 (d, J = 8.0 Hz, 1H, ArH); ^{13}C NMR (CDCl$_3$) δ (ppm): 18.3, 28.3, 36.7, 36.4, 40.6, 42.4, 44.1, 47.7, 48.8, 48.9, 49.2, 118.4, 123.0, 126.4, 127.0, 128.0, 128.4, 129.2, 129.3, 130.4, 132.7, 136.4, 137.7, 139.1, 153.1, 169.0, 170.3, 172.0, 172.2. Elem. Anal. for C$_{32}$H$_{34}$N$_4$O$_7$, calcd C 65.52, H 5.84, N 9.55, found C 63.88, H 6.00, N 9.64; ESI-MS m/z 587.2 (M + H)$^+$, calcd 587.2.

3. ^{1}H NMR (8:2 DMSO-d_6/H$_2$O, 400 MHz) δ (ppm): 1.89 (m, 1H, PyrrolidineH-4$_{cis}$), 1.92 (m, 1H, PyrrolidineH-4$_{trans}$), 2.00 (m, 1H, PyrrolidineH-4$_{cis}$), 2.06 (m, 1H, PyrrolidineH-4$_{trans}$), 2.22 (s, 3H, CH$_3$), 2.39 (m, 1H, AspHβ), 2.72 (m, 1H, AspHβ), 2.91 (m, 1H, PyrrolidineH-3$_{trans}$), 2.96 (m, 1H, PyrrolidineH-3$_{cis}$), 3.21 (m, 1H, PyrrolidineH-5$_{cis}$), 3.28 (m, 1H, PyrrolidineH-2$_{trans}$), 3.39–3.45 (m, 3H, PyrrolidineH-5$_{trans}$ + NCH$_2$Ar), 3.45 (m, 1H, PyrrolidineH-5$_{cis}$), 3.54 (m, 1H, PyrrolidineH-2$_{cis}$), 3.56 (m, 1H, PyrrolidineH-2$_{trans}$), 3.63 (m, 1H, PyrrolidineH-5$_{trans}$), 3.75 (t, J = 8.8 Hz, 1H, PyrrolidineH-2$_{cis}$), 4.19 (s, 2H, PhCH$_2$CO$_{cis}$), 4.21 (s, 2H, PhCH$_2$CO$_{trans}$), 4.75 (m, 1H, AspHα$_{cis}$), 4.81 (m, 1H, AspHα$_{trans}$), 6.93 (t, J = 7.2 Hz, 1H, ArH$_4$), 7.09–7.18 (m, 4H, ArH$_{3,5}$ + ArH$_{3',5'}$), 7.16–7.28 (m, 5H, PhCH$_2$CON), 7.39 (d, J = 8.4 Hz, 2H, ArH$_{2',6'}$), 7.81 (d, J = 8.0 Hz, 1H, ArH$_6$), 7.89 (s, 1H, NHa), 8.43 (br.t, 1H, NHc$_{trans}$), 8.46 (br.t, 1H, NHc$_{cis}$), 8.54 (br.d, 1H, AspNH$_{trans}$), 8.56 (br.d, 1H, AspNH$_{cis}$), 8.98 (s, 1H, NHb); ^{13}C NMR (DMSO-d_6) δ (ppm): 18.3, 28.3, 29.9, 39.4, 40.2, 42.4, 44.1, 45.8, 46.0, 47.4, 48.8, 48.9, 49.2, 118.4, 121.5, 126.4, 126.6, 127.8, 128.4, 129.3, 130.4, 132.7, 133.0, 136.4, 137.7, 139.1, 153.1, 168.8, 170.3, 171.7, 172.0. Elem. Anal. for C$_{32}$H$_{35}$N$_5$O$_6$, calcd C 65.63, H 6.02, N 11.96, found C 66.20, H 6.18, N 11.70; ESI-MS m/z 586.2 (M + H)$^+$, calcd 586.3.

4. ^{1}H NMR (8:2 DMSO-d_6/H$_2$O, 400 MHz) δ (ppm): 1.85 (m, 1H, PyrrolidineH-4$_{cis}$), 1.95–2.05 (m, 2H, PyrrolidineH-4$_{trans}$ + PyrrolidineH-4$_{cis}$), 2.15 (m, 1H, PyrrolidineH-4$_{trans}$), 2.18 (s, 3H, CH3), 2.57 (m, 1H, AspHβ), 2.94 (m, 1H, AspHβ), 2.97 (m, 1H, PyrrolidineH-3$_{trans}$), 3.22 (dd, J = 6.0, 10.0 Hz, 1H, PyrrolidineH-5$_{cis}$), 3.39–3.48 (m, 4H, PyrrolidineH-3$_{cis}$ + NCH$_2$Ar + PyrrolidineH-2$_{trans}$), 3.49–3.55 (m, 3H, PyrrolidineH-5$_{trans}$ + PyrrolidineH-5$_{cis}$ + PyrrolidineH-2$_{trans}$), 3.58 (m, 1H, PyrrolidineH-5$_{trans}$), 4.21 (d, J = 6.0 Hz, 2H, PhCH$_2$CO), 4.34 (dd, J = 4.8, 8.8 Hz, 1H, PyrrolidineH-2$_{cis}$), 4.43 (t, J = 9.2 Hz, 1H, PyrrolidineH-2$_{cis}$), 4.59 (m, 1H, AspHα$_{cis}$), 4.63 (m, 1H, AspHα$_{trans}$), 6.90 (t, J = 7.2 Hz, 1H, ArH4), 7.10–7.19 (m, 4H, ArH$_{3,5}$ + ArH$_{3',5'}$), 7.13–7.24 (m, 5H, ArH″), 7.40 (d, J = 8.2 Hz, 2H, ArH$_{2',6'}$), 7.79 (d, J = 8.0 Hz, 1H, ArH6), 7.90 (s, 1H, NHa), 8.41 (br.t, 1H, NHc$_{trans}$), 8.45 (br.t, 1H, NHc$_{cis}$), 8.50 (br.d, 1H, AspNH$_{trans}$), 8.54 (br.d, 1H, AspNH$_{cis}$), 8.91 (s, 1H, NHb); ^{13}C NMR (DMSO-d_6, 400 MHz) δ (ppm): 18.3, 28.3, 29.5, 29.9, 39.4, 42.4, 42.7, 44.1, 45.0, 47.7, 48.2, 49.2, 55.0, 118.4, 121.5, 126.4, 127.8, 128.4, 129.2, 129.3, 130.4, 132.7, 136.4, 137.7, 139.1, 153.1, 171.7, 172.0, 172.2, 172.3. Elem. Anal. for C32H35N5O6, calcd C 65.63, H 6.02, N 11.96, found: C 66.94, H 6.19, N 11.72; ESI-MS m/z 586.1 (M + H)$^+$, calcd 586.3.

5. ^{1}H NMR (DMSO-d_6, 400 MHz) δ (ppm): (two sets of resonances: ≥major conformer; ≤minor conformer) 2.00–2.18 (m, 2H, PyrrolidineH-4$_<$), 2.20–2.38 (m, 2H, PyrrolidineH-4$_>$), 2.39 (s, 3H, CH$_3$Ph), 2.58 (m, 1H, AspHβ), 2.90 (m, 1H, PyrrolidineH-3$_>$), 2.98 (m, 1H, AspHβ), 3.08 (m, 1H, PyrrolidineH-3$_<$), 3.35 (m, 1H, Proδ$_<$), 3.46 (dd, J = 8.0, 12.0 Hz, 1H, Proα$_>$), 3.59 (m, 2H, PyrrolidineH-5$_<$ + PyrrolidineH-5$_>$), 3.70 (dd, J = 8.0, 12.0 Hz, 1H, Proα$_>$), 3.79 (dd, J = 7.6, 9.2 Hz, 1H, Proα$_<$), 4.00 (m, 1H, Proδ$_>$), 4.09 (m, 1H, Proα$_<$), 4.24 (d, J = 5.6 Hz, 2H, CH$_2$Ph), 5.12 (m, 1H, AspHα), 6.81 (t,

J = 7.6 Hz, 1H, ArH), 7.02–7.14 (m, 4H, ArH), 7.15–7.26 (m, 3H, ArH), 7.35 (t, J = 8.4 Hz, 2H, ArH), 7.58 (s, 1H, NH), 7.79 (d, J = 8.4 Hz, 1H, ArH), 7.81 (br.t, 1H, NH$_>$), 7.85 (br.t, 1H, NH$_<$), 8.40 (d, J = 7.6 Hz, 1H, AspNH$_<$), 8.55 (d, J = 7.6 Hz, 1H, AspNH$_>$), 8.62 (s, 1H, NH$_>$), 8.64 (s, 1H, NH$_<$). Elem. Anal. for C$_{31}$H$_{31}$Cl$_2$N$_5$O$_6$, calcd C 58.13, H 4.88, N 10.93, found C 57.00, H 4.81, N 10.15; ESI-MS m/z 640.1 (M + H)$^+$, calcd 640.2.

6. ^{1}H NMR (DMSO-d_6, 400 MHz) δ (ppm): (two sets of resonances: ≥major conformer; ≤minor conformer) 1.95 (m, 2H, PyrrolidineH-4$_<$), 2.05 (m, 2H, PyrrolidineH-4$_>$), 2.29 (s, 3H, CH$_3$Ph), 2.56 (m, 1H, AspHβ), 2.92–2.98 (m, 2H, PyrrolidineH-3 + AspHβ), 3.25 (m, 1H, Proδ$_<$), 3.47 (m, 1H, PyrrolidineH-2$_>$), 3.60 (m, 2H, PyrrolidineH-5$_<$ + PyrrolidineH-5$_>$), 3.69–3.79 (m, 2H, Proα$_>$ + Proα$_<$), 3.99 (m, 1H, Proδ$_>$), 4.11 (m, 1H, Proα$_<$), 4.27 (br.s, 2H, CH$_2$Ph), 5.09 (m, 1H, AspHα), 6.81 (br.t, 1H, ArH), 7.01–7.14 (m, 4H, ArH), 7.15–7.26 (m, 3H, ArH), 7.27–7.35 (m, 2H, ArH), 7.52 (s, 1H, NH), 7.70 (d, J = 8.4 Hz, 1H, ArH), 7.75 (br.t, 1H, NH$_>$), 7.81 (br.t, 1H, NH$_<$), 8.20 (br.d, 1H, AspNH$_<$), 8.25 (br.d, 1H, AspNH$_>$), 8.51 (s, 1H, NH); ^{13}C NMR (CDCl$_3$) δ (ppm): 18.2, 28.4, 29.5, 39.4, 42.7, 48.7, 49.0, 51.2, 118.6, 121.8, 124.1, 127.0, 128.6, 129.5, 131.0, 131.4, 132.8, 133.8, 136.6, 136.8, 138.0, 153.4, 167.4, 171.2, 172.0, 173.1. Elem. Anal. for C$_{31}$H$_{31}$Cl$_2$N$_5$O$_6$, calcd C 58.13, H 4.88, N 10.93, found C 57.60, H 4.79, N 11.13; ESI-MS m/z 640.1 (M + H)$^+$, calcd 640.2.

4.3. Scintillation proximity-binding assay (SPA)

We developed a SPA assay to detect competitive binding of drugs to soluble ^{125}I-human FN (Mw approximately 440 kDa) bound to an antibody-captured integrin complex [46,47]. The assay uses microspheres coated with an anti-rabbit IgG antibody capable of binding the complex α$_4$ integrin anti-α$_4$ antibody. The radioligand binds to the α$_4$β$_1$ integrin and the close proximity of the isotope to the scintillant incorporated in the beads allows the radiation energy to transfer to the scintillant where it can be detected as counts per min (cpm). The procedure is described in detail in S.M.

4.4. Adhesion assays

Jurkat cell adhesion assays were done as described [46,47]. Briefly, 96-well plates were coated at 4 °C overnight with 2 mg/mL of VCAM-1 and a saturation curve for the ligand was plotted to establish the best signal-to-noise ratio. Non-specific hydrophobic binding sites were blocked by incubation with a BSA (1%)/HBSS (w/v) solution for 30 min at 37 °C. SK-MEL-24 cell adhesion assays were done as described [44]. The procedure is described in detail in S.M.

4.5. Data analysis

All data are expressed as mean ± S.E.M., for the number of experiments indicated. SPA binding data and ligand concentration–response curves were analyzed using GraphPad software (Graph-Pad Software Inc., San Diego, CA, USA). IC$_{50}$ values indicate the molar ligand concentration required to inhibit the response by 50% and were converted, in SPA experiments, to Ki values using the method of Cheng and Prusoff [54].

4.6. In vitro metabolic stability

Enzymatic degradation studies of **1**, **3**, and **4** were carried out in triplicate and repeated three times using mouse serum purchased from Sigma–Aldrich. Peptides were dissolved in Tris buffer pH 7.4 and 10 μL aliquots of a 10 mM peptide stock solution were added to 190 μL of serum. Incubations were carried out at 37 °C for 120 min.

Aliquots of 20 μL were withdrawn from the incubation mixtures and enzyme activity was terminated by precipitating proteins with 90 μL of glacial acetonitrile. Samples were then diluted with 90 μL of 0.5% acetic acid to prevent further enzymatic breakdown and centrifuged at 13,000×g for 15 min. The supernatants were collected and the stability of peptides was determined by RP-HPLC ESI-MS analysis.

4.7. Conformational analysis

The unambiguous assignment of ^{1}H NMR resonances was performed by 2D gCOSY. 2D ROESY experiments were recorded in 8:2 DMSO-d_6/H$_2$O, with a 250 ms mixing time with a proton spectral width of 3088 Hz. Peaks were calibrated on DMSO. Only ROESY-derived constraints (force constant: 7 kcal mol^{-1} Å^{-2}) were included in the restrained molecular dynamics. Cross-peak intensities were classified very strong, strong, medium, and weak, and were associated with distances of 2.2, 2.6, 3.0, and 4.5 Å, respectively. Geminal couplings and other obvious correlations were discarded. The ω bonds were set at 180° (16 kcal mol^{-1} Å^{-2}). The restrained MD simulations were conducted using the AMBER force field in a 45 × 45 × 45 Å box of standard TIP3P models of equilibrated water. The procedure is described in detail in S.M.

Acknowledgments

Appendix A. Supplementary material

Supplementary material related to this article can be found at http://dx.doi.org/10.1016/j.ejmech.2013.12.009.

References

[1] D.M. Rose, R. Alon, M.H. Ginsberg, Integrin modulation and signaling in leukocyte adhesion and migration, Immunol. Rev. 218 (2007) 126–134.
[2] J. Singh, S. Adams, M.B. Carter, H. Cuervo, W.C. Lee, R.R. Lobb, R.B. Pepinsky, R. Petter, D. Scott, Rational design of potent and selective VLA-4 inhibitors and their utility in the treatment of asthma, Curr. Top. Med. Chem. 4 (2004) 1497–1507.
[3] P. Vanderslice, D.G. Woodside, Very late activation antigen-4 (VLA-4) antagonist, Prog. Respir. Res. 39 (2010) 169–173.
[4] R. Gonzalez-Amaro, M. Mittelbrunn, F. Sanchez-Madrid, Therapeutic anti-integrin (α4 and αL) monoclonal antibodies: two-edged swords? Immunology 116 (2005) 289–296.
[5] P.S. Rommer, R. Patejdl, U.K. Zettl, Monoclonal antibodies in the treatment of neuroimmunological diseases, Curr. Pharm. Des. 18 (2012) 4498–4507.
[6] D.Y. Jackson, Alpha 4 integrin antagonists, Curr. Pharm. Des. 8 (2002) 1229–1253.
[7] G.X. Yang, W.K. Hagmann, VLA-4 antagonists: potent inhibitors of lymphocyte migration, Med. Res. Rev. 23 (2003) 369–392.
[8] K. Lin, H.S. Ateeq, S.H. Hsiung, L.T. Ching, C.N. Zimmerman, A. Castro, W.C. Lee, C.E. Hammond, S. Kalkunte, L.L. Chen, R.B. Pepinsky, D.R. Leone, A.G. Sprague, W.M. Abraham, A. Gill, R.R. Lobb, S.P. Adams, Selective, tight-binding inhibitors of integrin α4β1 that inhibit allergic airway responses, J. Med. Chem. 42 (1999) 920–934.
[9] G.T. Bolger, BIO-1211 (Biogen), IDrugs 3 (2000) 536–540.
[10] P.C. Astles, N.V. Harris, A.D. Morley, Diamine containing VLA-4 antagonists, Bioorg. Med. Chem. 9 (2001) 2195–2202.
[11] B.V. Karanam, A. Jayra, M. Rabe, Z. Wang, C. Keohane, J. Strauss, S. Vincent, Effect of enalapril on the in vitro and in vivo peptidyl cleavage of a potent VLA-4 antagonist, Xenobiotica 37 (2007) 487–502.
[12] A.L. Fisher, E. DePuy, A. Jayaraj, C. Raab, M. Braun, M. Ellis-Hutchings, J. Zhang, J.D. Rogers, D.G. Musson, LC/MS/MS plasma assay for the peptidomimetic VLA4 antagonist I and its major active metabolite II: for treatment of asthma by inhalation, J. Pharm. Biomed. Anal. 27 (2002) 57–71.
[13] J. Singh, H. Van Vlijmen, Y. Liao, W.C. Lee, M. Cornebise, M. Harris, I. Shu, A. Gill, J.H. Cuervo, W.M. Abraham, S.P. Adams, Identification of potent and

[14] I. Sircar, K.S. Gudmundsson, R. Martin, J. Liang, S. Nomura, H. Jayakumar, B.R. Teegarden, D.M. Nowlin, P.M. Cardarelli, J.R. Mah, S. Connell, R.C. Griffith, E. Lazarides, Synthesis and SAR of N-benzoyl-L-biphenylalanine derivatives: discovery of TR-14035, a dual α4β7/α4β1 integrin antagonist, Bioorg. Med. Chem. 10 (2002) 2051–2066.
[15] M. Barczyk, S. Carracedo, D. Gullberg, Integrins, Cell Tissue Res. 339 (2010) 269–280.
[16] A.P. Mould, A. Komoriya, K.M. Yamada, M.J. Humphries, The CS5 peptide is a second site in the IIICS region of fibronectin recognized by the integrin alpha 4 beta 1. Inhibition of alpha 4 beta 1 function by RGD peptide homologues, J. Biol. Chem. 266 (1991) 3579–3585.
[17] P.M. Cardarelli, R.R. Cobb, D.M. Nowlin, W. Scholz, F. Gorcsan, M. Moscinski, M. Yasuhara, S.L. Chiang, T.J. Lobl, Cyclic RGD peptide inhibits alpha 4 beta 1 interaction with connecting segment 1 and vascular cell adhesion molecule, J. Biol. Chem. 269 (1994) 18668–18673.
[18] D.M. Nowlin, F. Gorcsan, M. Moscinski, T. Chiang, T.J. Lobl, P.M. Cardarelli, A novel cyclic pentapeptide inhibits α4β1 and α5β1 integrin-mediated cell adhesion, J. Biol. Chem. 268 (1993) 20352–20359.
[19] D.Y. Jackson, C. Quan, D.R. Artis, T. Rawson, B. Blackburn, M. Struble, G. Fitzgerald, K. Chan, S. Mullins, J.P. Burnier, W.J. Fairbrother, K. Clark, M. Berisini, H. Chui, M. Renz, S. Jones, S. Fong, Potent α4β1 peptide antagonists as potential anti-inflammatory agents, J. Med. Chem. 40 (1997) 3359–3368.
[20] S. Elitok, S.V. Brodsky, D. Patschan, T. Orlova, K.M. Lerea, P. Chander, M.S. Goligorsky, Cyclic arginine-glycine-aspartic acid peptide inhibits macrophage infiltration of the kidney and carotid artery lesions in apo-E-deficient mice, Am. J. Physiol. Renal. Physiol. 290 (2006) F159–F166.
[21] C. Henry, N. Moitessier, Y. Chapleur, Vitronectin receptor -αVβ3 integrin-antagonists: chemical and structural requirements for activity and selectivity, Mini Rev. Med. Chem. 2 (2002) 531–542.
[22] A. Perdih, M. Sollner Dolenc, Small molecule antagonists of integrin receptors, Curr. Med. Chem. 17 (2010) 2371–2392.
[23] J. Wermuth, S.L. Goodman, A. Jonczyk, H. Kessler, Stereoisomerism and biological activity of the selective and superactive αvβ3 integrin inhibitor cyclo(-RGDfV-) and its retro-inverso peptide, J. Am. Chem. Soc. 119 (1997) 1328–1335.
[24] L. Gentilucci, G. Cardillo, S. Spampinato, A. Tolomelli, F. Squassabia, R. De Marco, A. Bedini, M. Baiula, L. Belvisi, M. Civera, Antiangiogenic effect of dual/selective α5β1/αvβ3 integrin antagonists designed on partially modified retro-inverso cyclotetrapeptide mimetics, J. Med. Chem. 53 (2010) 106–118.
[25] A.O. Frank, E. Otto, C. Mas-Moruno, H.B. Schiller, L. Marinelli, S. Cosconati, A. Bochen, D. Vossmeyer, G. Zahn, R. Stragies, E. Novellino, H. Kessler, Conformational control of integrin-subtype selectivity in isoDGR peptide motifs: a biological switch, Angew. Chem. Int. Ed. 49 (2010) 9278–9281.
[26] A. Bochen, U.K. Marelli, E. Otto, D. Pallarola, C. Mas-Moruno, F.S. Di Leva, H. Boehm, J.P. Spatz, E. Novellino, H. Kessler, L. Marinelli, Biselectivity of isoDGR peptides for fibronectin binding integrin subtypes α5β1 and αvβ6: conformational control through flanking amino acids, J. Med. Chem. 56 (2013) 1509–1519.
[27] F. Curnis, R. Longhi, L. Crippa, A. Cattaneo, E. Donossola, E. Bachi, A. Corti, Spontaneous formation of L-isoaspartate and gain of function in fibronectin, J. Biol. Chem. 281 (2006) 36466–36476.
[28] V. Takahashi, M. Leiss, M. Moser, T. Ohashi, T. Kitao, D. Heckmann, A. Pfeifer, H. Kessler, J. Takagi, H.P. Erickson, R. Fässler, The RGD motif in fibronectin is essential for development but dispensable for fibril assembly, J. Cell Biol. 178 (2007) 167–178.
[29] J. Xu, L.M. Maurer, B.R. Hoffmann, D.S. Annis, D.F. Mosher, iso-DGR sequences do not mediate binding of fibronectin N-terminal modules to adherent fibronectin-null fibroblasts, J. Biol. Chem. 285 (2010) 8563–8571.
[30] A. Spitaleri, M. Ghitti, S. Mari, L. Alberici, C. Traversari, G.P. Rizzardi, G. Musco, Use of metadynamics in the design of isoDGR-based αvβ3 antagonists to fine-tune the conformational ensemble, Angew. Chem. Int. Ed. 50 (2011) 1832–1836.
[31] M. Ghitti, A. Spitaleri, B. Valentinis, S. Mari, C. Asperti, C. Traversari, G.P. Rizzardi, G. Musco, Molecular dynamics reveal that isoDGR-containing cyclopeptides are true αvβ3 antagonists unable to promote integrin allostery and activation, Angew. Chem. Int. Ed. 51 (2012) 7702–7705.
[32] M. Mingozzi, A. Dal Corso, M. Marchini, I. Guzzetti, M. Civera, U. Piarulli, D. Arosio, L. Belvisi, D. Potenza, L. Pignataro, C. Gennari, Cyclic isoDGR peptidomimetics as low-nanomolar αvβ3 integrin ligands, Chem. Eur. J. 19 (2013) 3563–3567.
[33] J. Singh, H. van Vlijmen, W.C. Lee, Y. Liao, K.C. Lin, H. Ateeq, J. Cuervo, C. Zimmerman, C. Hammond, M. Karpusas, R. Palmer, T. Chattopadhyay, S.P. Adams, 3D QSAR (COMFA) of a series of potent and highly selective VLA-4 antagonists, J. Comput. Aided Mol. Des. 16 (2002) 201–211.
[34] S. Thangapandian, S. John, S. Sakkiah, K.W. Lee, Discovery of potential integrin VLA-4 antagonists using pharmacophore modeling, virtual screening and molecular docking studies, Chem. Biol. Drug Des. 78 (2011) 289–300.
[35] HyperChem Release 8.0.3, Hypercube Inc. 1115 NW 4th St. Gainesville, FL 32608 (USA), 2012.
[36] J. Witherington, V. Bordas, A. Gaiba, P.M. Green, A. Naylor, N. Parr, D.G. Smith, A.K. Taklea, R.W. Ward, Pyridone derivatives as potent and selective VLA-4 integrin antagonists, Bioorg. Med. Chem. Lett. 16 (2006) 2256–2259.

[37] L. Gentilucci, R. De Marco, L. Cerisoli, Chemical modifications designed to improve peptide stability: incorporation of non-natural amino acids, pseudo-peptide bonds, and cyclization, Curr. Pharm. Des. 16 (2010) 3185–3203.

[38] B.R. Huck, J.M. Langenhan, S.H. Gellman, Non-hydrogen-bonded secondary structure in β-peptides: evidence from circular dichroism of (S)-pyrrolidine-3-carboxylic acid oligomers and (S)-nipecotic acid oligomers, Org. Lett. 1 (1999) 1717–1720.

[39] L.M. Sandvoss, H.A. Carlson, Conformational behavior of β-proline oligomers, J. Am. Chem. Soc. 125 (2003) 15855–15862.

[40] G. Lelais, D. Seebach, β²-Amino acids-syntheses, occurrence in natural products, and components of β-peptides, Biopolymers 76 (2004) 206–243.

[41] E. Juaristi, V. Soloshonok (Eds.), Enantioselective Synthesis of β-Amino Acids, second ed., Wiley-VCH, New York, 2005.

[42] A. Tolomelli, L. Gentilucci, E. Mosconi, A. Viola, E. Paradisi, A straightforward route to enantiopure 2-substituted-3,4-dehydro-β-proline via ring closing metathesis, Amino Acids 41 (2011) 575–586.

[43] G. Cardillo, L. Gentilucci, A. Tolomelli, M. Calienni, A.R. Qasem, S. Spampinato, Stability against enzymatic hydrolysis of endomorphin-1 analogues containing β-proline, Org. Biomol. Chem. 1 (2003) 1498–1502.

[44] A. Tolomelli, L. Gentilucci, E. Mosconi, A. Viola, S.D. Dattoli, M. Baiula, S. Spampinato, L. Belvisi, M. Civera, Development of isoxazoline-containing peptidomimetics as dual αvβ3 and α5β1 integrin ligands, ChemMedChem 6 (2011) 2264–2272.

[45] A. Macchiarulo, G. Costantino, M. Meniconi, K. Pleban, G. Ecker, D. Bellocchi, R. Pellicciari, Insights into phenylalanine derivatives recognition of VLA-4 integrin: from a pharmacophoric study to 3D-QSAR and molecular docking analyses, J. Chem. Inf. Comput. Sci. 44 (2004) 1829–1839.

[46] A.R. Qasem, C. Bucolo, M. Baiula, A. Spartà, P. Govoni, A. Bedini, D. Fascì, S. Spampinato, Contribution of α4β1 integrin to the antiallergic effect of lev-ocabastine, Biochem. Pharmacol. 76 (2008) 751–762 and references herein.

[47] C. Solorzano, S. Bouquelet, M.A. Pereyra, F. Blanco-Favela, M.C. Slomianny, R. Chavez, R. Lascurain, E. Zenteno, C. Algundis, Isolation and characterization of the potential receptor for wheat germ agglutinin from human neutrophils, Glycoconj. J. 23 (2006) 591–598.

[48] A. Bedini, M. Baiula, L. Gentilucci, A. Tolomelli, R. De Marco, S. Spampinato, Peripheral antinociceptive effects of the cyclic endomorphin-1 analog c [YpwFG] in a mouse visceral pain model, Peptides 31 (2010) 2135–2140.

[49] PyrrolidineH-2 and H-5 correspond to β-ProHα and β-ProHδ, respectively, in the following paper: A. Katarzyńska, M. Bilska, E. Adamek, M. Zimecki, S. Jankowski, J. Zabrocki, Synthesis and immunosuppressive activity of new cyclolinopeptide A analogs modified with β-prolines J. Pept. Sci. 14 (2008) 1283–1294.

[50] P.A. Temussi, D. Picone, G. Saviano, P. Amodeo, A. Motta, T. Tancredi, S. Salvadori, R. Tomatis, Conformational analysis of an opioid peptide in sol-vent media that mimic cytoplasm viscosity, Biopolymers 32 (1992) 367–372 and references herein.

[51] A. Borics, G. Tóth, Structural comparison of μ-opioid receptor selective pep-tides confirmed four parameters of bioactivity, J. Mol. Graph. Model. 28 (2010) 495–505.

[52] For a molecular docking analysis, see: T.J. You, D.S. Maxwell, T.P. Kogan, Q. Chen, J. Li, J. Kassir, G.W. Holland, R.A.F. Dixon, A 3D structure model of integrin α4β1 complex: I. Construction of a homology model of β1 and ligand binding analysis Biophys. J. 82 (2002) 447–457.

[53] Also on molecular docking: C.M. Carlevaro, J.H.M. Da Silva, W. Savino, E.R. Caffarena, Plausible binding mode of the active α4β1 antagonist, Mk-0617, determined by docking and free energy calculations J. Theor. Comput. Chem. 12 (2013) 1250108/1–16.

[54] Y. Cheng, W.H. Prusoff, Relationship between the inhibition constant (Ki) and the concentration of inhibitor which causes 50 per cent inhibition (I50) of an enzymatic reaction, Biochem. Pharmacol. 22 (1973) 3099–3108.